On the measurement of hardness in coal

Characterization of the hardness of coal is difficult for two reasons. The first is that this "organic rock" has a complex heterogeneous microstructure, which makes it difficult to place successive indentations at structurally equivalent sites. The problem is not merely that coal consists of composite layers (microlithotypes) of one or more distinct organic constituents (macerals) laid down parallel to the bedding plane, but also that individual macerals (i) are non-uniform in structure, composition and properties and (ii) contain inorganic inclusions, cracks and micropores (which last frequently contain substantial amounts of physi- and/or chemisorbed moisture). The second cause of difficulty is that individual macerals can either be very brittle or deform in a manner that is predominantly reversible rather than permanent. In the former instance cracking and chipping around and beneath the indenter can produce ill-defined indentations; and in the latter case extensive elastic and/or anelastic recovery during unloading can produce a misleading result.

In consequence, it has been usual to measure only the conventional low-load (15 to 500 g) Vickers microhardness of single maceral regions* of polished surfaces oriented perpendicular to the bedding plane or the higher load (1000 to 2000 g) "Vickers macrostrength" of particular bi- or tri-maceral microlithotypes in similarly prepared and oriented sections [1]. Moreover, in order to make indentations more visible and to better estimate their size prior to unloading, it is common to coat the surfaces of specimens with soot prior to testing [1]. Hence, past studies have provided little or no indication of how hardness varies either from one maceral to another or with orientation relative to the bedding plane. Nor have they made clear what effect soot coating a surface has on its measured hardness. The purpose of this investigation was to explore these questions, and to this end three series of Vickers microhardness measurements have been made.

The first series used as test materials the five coals listed in Table I. Rectangular slabs, oriented either parallel or perpendicular to the bedding plane and approximately 2 cm x 2 cm x 2 cm in size, were cut from larger blocks of each coal with a water-cooled diamond saw, mounted in Koldmount† self-curing resin, rough ground on a series of wet SiC papers down through 600 grit, and then given a final two-stage polish on Buehler‡ AB Rayvel cloth using aqueous slurries of 0.3 and 0.05 μm Al_2O_3 abrasive. The semianthracite specimens alone were then coated with soot by holding them over the smoky flame of a paraffin wax candle for a few seconds. Thereafter, each specimen was indented 20 times at randomly chosen sites and 10 times in vitrite regions, except that the semianthracite could only be indented randomly as a result of being coated.

TABLE I

Geographic location	Seam	Supplier	Apparent rank[a]	Fixed carbon (dry, mineral matter-free) (wt %)	Calorific value (moist, mineral matter-free) (cal g^{-1})
Appalachian	Shamokin, PA.	Glen Burn Colliery	Semianthracite	91.6	8247
Appalachian	Lower Freeport	PA. Power and Light Co.	Medium volatile bituminous	70.0	8734
Mid-Continent	West KY. No. 9	Midway Coal Co.	High volatile A bituminous	59.2	8025
Appalachian	OH. No. 9	Conoco Coal Co.	High volatile A bituminous	56.1	8181
Western	Belle Ayre South, WY.	Amax Coal Co.	Sub-bituminous B	56.8	5385

[a]According to ASTM Standard No. D 388-66 (1972).

*Strictly speaking, most of these measurements have been made in the pseudo-monomaceral microlithotype vitrite, which by definition contains > 95 vol % vitrinite. This is because vitrite, the dominant microlithotype of the coals of the Northern hemisphere, is the one microstructural constituent that regularly occurs in sufficiently large and defect-free regions.

†Vernon-Benshoff Company, 413 North Pearl Street, Albany 1, New York, USA.

‡Buehler Ltd., 2120 Greenwood Street, Evanston, Illinois 60204, USA.

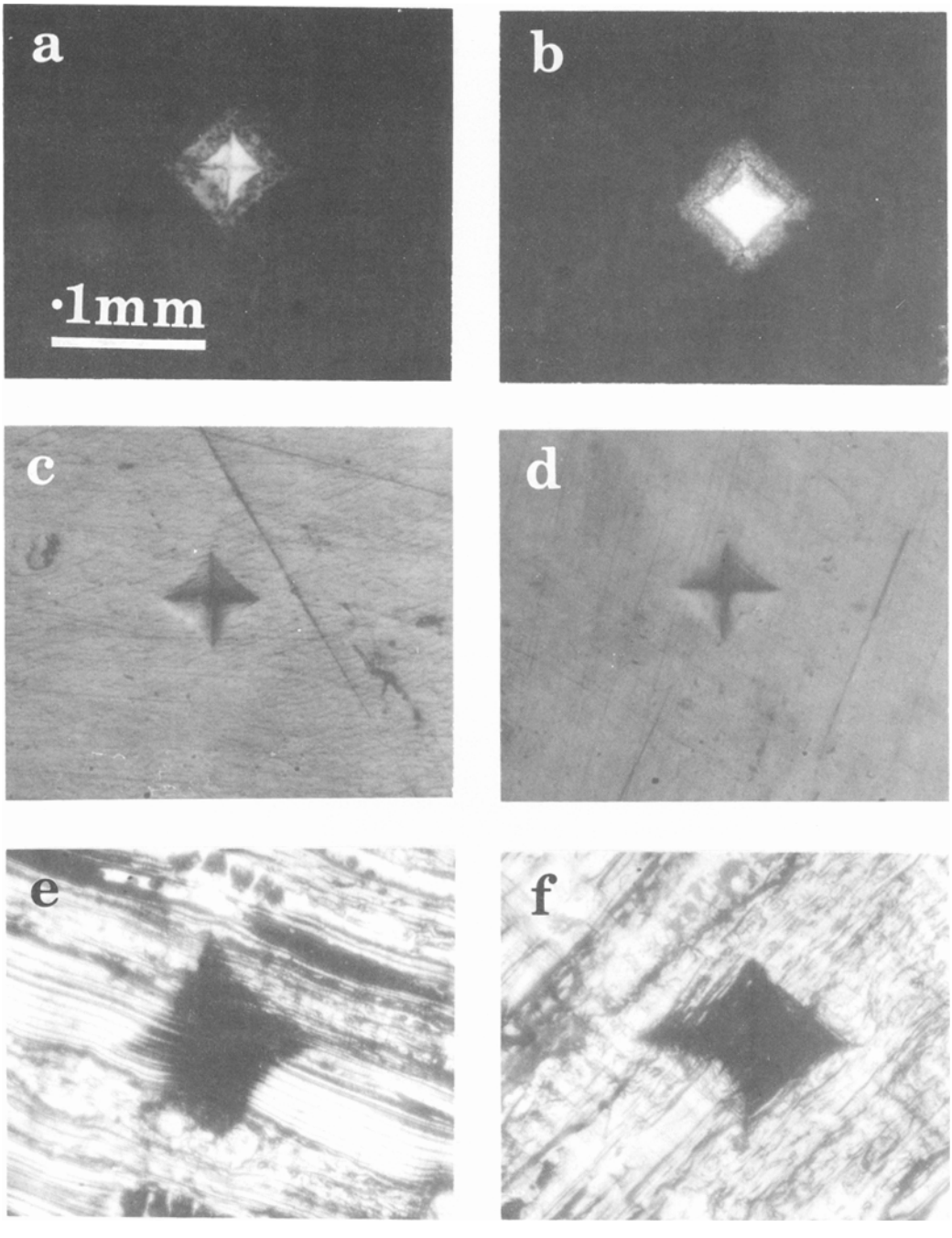

Figure 1 Vickers indentations (100 g load) on surfaces perpendicular and parallel to the bedding plane in various coals: semianthracite (a) ⊥ (b) ∥; high volatile bituminous (Conoco) (c) ⊥ (d) ∥; sub-bituminous (e) ⊥ (d) ∥.

TABLE II

Coal	Vickers hardness ($kg\,mm^{-2}$)			
	Surfaces ∥ bedding plane		Surfaces ⊥ bedding plane	
	In vitrite	At random	In vitrite	At random
Semianthracite, Glen Burn Colliery (soot-coated)	—	52.0 ± 2.4	—	54.0 ± 4.3
Medium volatile bituminous, PA. Power and Light Co.	32.6 ± 2.1	32.1 ± 6.7	35.2 ± 3.0	32.8 ± 3.3
High volatile A bituminous, Midway Coal Co.	29.7 ± 3.1	27.9 ± 5.0	29.7 ± 2.6	29.7 ± 2.6
High volatile A bituminous, Conoco Coal Co.	38.0 ± 1.2	40.8 ± 4.6	43.3 ± 4.4	38.7 ± 3.4
Sub-bituminous B, Amax Coal Co.	—	10.1 ± 1.5	—	9.3 ± 1.5

Each indentation was made using a load of 100 g and a loading time of 15 sec. Typical indentations are shown in Fig. 1, and the mean Vickers hardness numbers obtained are reported in Table II, together with their standard deviations. Separate studies on the high volatile A bituminous (Conoco) coal showed that neither keeping the load fixed at 100 g and increasing the loading time to 30 or 60 sec, nor varying the load from 50 to 250 g at a constant loading time of 15 sec, produced any clearly significant effect on the measured hardness.

The second series of indentations was made at randomly selected sites on the surface of a sample of the medium volatile bituminous coal. This sample was oriented perpendicular to the bedding plane, and was mounted and polished as described above before having one half of its surface coated with soot. 20 indentations were made on each half at each of three loads (25, 100 and 250 g), using throughout a loading time of 15 sec. Typical indentations from both regions are shown in Fig. 2,

TABLE III

Load (g)	Vickers hardness of medium volatile bituminous coal, ($kg\,mm^{-2}$)	
	With soot	No soot
25	62.7 ± 21.4	59.5 ± 17.0
100	28.3 ± 2.5	32.8 ± 3.3
250	32.4 ± 8.0	33.4 ± 5.9

and the results of the tests are summarized in Table III.

The final series of indentations was made on three materials – 2024-T351 Al alloy, soda-lime glass* and Koldmount self-curing resin – which, because they exhibit different values of yield strength/Young's modulus, may be expected to show different amounts of recovery upon unloading. No surface preparation was done on the glass specimens, but the Al alloy samples were polished on SiC papers down to 600 grit and the

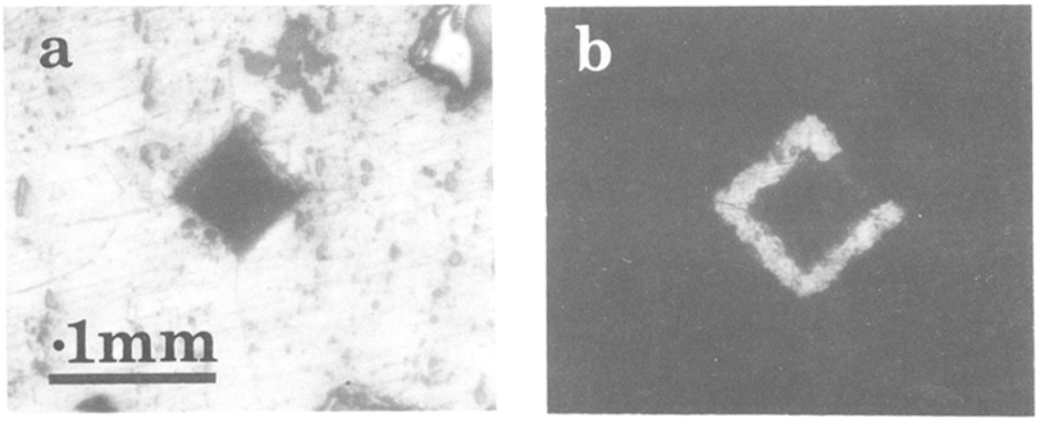

Figure 2 Vickers indentations (100 g load) in medium volatile bituminous coal on a surface perpendicular to the bedding plane: (a) uncoated; and (b) coated with soot.

*Type 2947 microscope slides from Corning Glass Works, Scientific Glassware Department, Corning, New York 14830, USA.

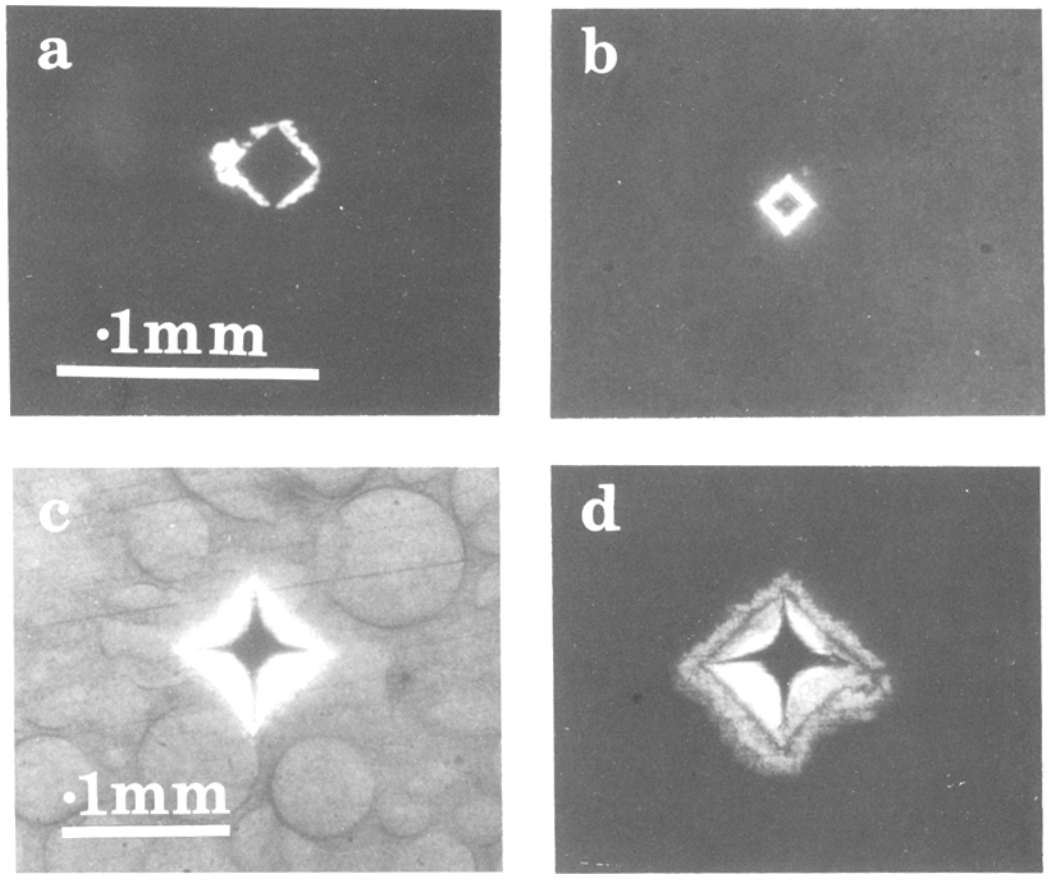

Figure 3 Vickers indentations (100 g load) on various materials with soot coatings: (a) Al alloy; (b) soda-lime glass [same magnification as (a)]; (c) Koldmount with a thin coating; (d) Koldmount with a thicker coating [same magnification as (c)].

Koldmount samples were prepared in the same manner as the coal specimens used in the previous two series of indentations. A load of 100 g and a loading time of 15 sec were used throughout, and 10 indentations were made in each material both before and after coating it with soot as described above. Typical indentations can be seen in Fig. 3, and the results are listed in Table IV.

Several conclusions can be drawn from the results of these three series of measurements. First, the examples in Fig. 1 and the data of Table II indicate that in none of the coals studied is there any significant difference between the hardness of a surface oriented perpendicular to the bedding plane and one parallel to it, regardless of the choice of load and loading time used in the measurement, and regardless of whether the indentations are placed in the dominant vitrite microlithotype or at random. Hence, despite the microstructural heterogeneity and anisotropy of the typical coal, its hardness can adequately be defined by a single number. Second, because the scatter in the hardness data obtained by indenting at random is small compared to the variation of hardness with rank (Table II), it is also apparent that the hardness of coal is influenced much more by the extent of coalification than by the nature of its precursors. The third conclusion that may be drawn from these results is that soot coatings have no significant effect on the hardness of either coal (Table III) or any other of the materials studied (Table IV), provided that the hardness is defined (as is conventional) in terms of the dimensions of the residual permanent indentation. It is also noteworthy that, regardless of whether it appears light or dark (i.e., of whether the soot compressed between the indenter and the substrate adheres to the former or the latter), an indentation made in

TABLE IV

Material	Vickers hardness ($kg\,mm^{-2}$)	
	With soot	No soot
2024-T351 Al alloy	172 ± 19	192 ± 6
Soda-lime glass	741 ± 80	710 ± 25
Koldmount resin	18.3 ± 0.9	20.4 ± 0.6

TABLE V

Material	Yield strength/ Young's modulus
2024-T351 Al alloy	$\sim 5 \times 10^{-3}$
Soda-lime glass	$\sim 4 \times 10^{-2}$
Koldmount resin	$\sim 2 \times 10^{-2}$
Medium volatile bituminous coal	$\sim 2 \times 10^{-2}$
Semianthracite	$\sim 3 \times 10^{-2}$

a more densely soot-covered specimen is surrounded by a "halo", the extent of which generally increases as the ratio of the yield strength of the substrate to its Young's modulus increases (See Table V and Figs. 1 to 3). Accordingly, it is suggested that this halo is the result of local disintegration of the soot film under the action of the elastic tensile stresses generated during indentation in the surface regions of the substrate immediately outside the area of contact with the indenter. Note, however, that the formation of such haloes can be supressed by reducing the thickness of the soot coating (Fig. 3).

Acknowledgement

The authors gratefully acknowledge the capable experimental assistance of Mr J. Kunkle in this work.

Reference

1. E. STACH, M.-Th. MACKOWSKY, M. TEICHMÜLLER, G. H. TAYLOR, D. CHANDRA and R. TEICHMÜLLER, "Stach's Textbook of Coal Petrology", (Gebrüder Borntraeger, Berlin and Stuttgart, 1975).

Received 21 April
and accepted 25 May 1978.

N. H. MACMILLAN
D. G. RICKERBY
Materials Research Laboratory,
The Pennsylvania State University,
University Park, Pa 16802, USA

Nucleation and growth of crazes in polycarbonate exposed to ethanol

In a previous publication the effect of ethanol on the environmental stress crazing of polycarbonate was described [1]. It was shown that both the nucleation and growth of crazes generated around a centrally located hole were controlled by the major principal strain. Photographic slides of the material being crazed, illustrations of which are shown in [1], were taken in time intervals of from 5 min to 9 h. Thus we have a record of the length of all crazes generated in the plates as a function of time.

It was found that new crazes initiated during the course of the experiment and that the frequency of craze nucleation was a function of time. Fig. 1 shows the average frequency of craze formation in a 3.2 mm thick polycarbonate plate containing a centrally located 12.7 mm diameter hole under a stress of 2.5 k.s.i. and exposed to ethanol.

The resultant distribution is not normal and, in fact, is highly skewed toward longer induction times. Since crazes nucleate at flaws, a craze that nucleates at a small flaw could grow for a long time before it reaches a "visible" size and is counted, while a craze emanating from a severe flaw might be detected much earlier.

A plot of the number of crazes formed as a function of time (Fig. 2) shows that the number of crazes first increases with time and then appears to reach a plateau. Continued exposure to solvent, however, appears to generate a new group of crazes after an additional induction period. Each craze appears to have a different growth rate and it is noted that some of the crazes show intermittant growth in which the crazes grow, arrest and then start to grow again. The reasons for these phenomena are not clear but it is known that crazes can interact with each other in a complex fashion.

Fig. 3 shows the total length of all crazes formed as a function of time, which is a measure of the cumulative damage in the sheet. The data plot to a straight line with a slope of one on log–log coordinates. The functional form is thus $x(t) = kt$, at least after a short initial period where it is